*34th EPS Conference on Plasma Phys. Warsaw, 2 - 6 July 2007 ECA Vol.**31F**, P-4.063 (2007)*

Calculations of an effective ripple for a stellarator magnetic field computed by the HINT2 code*

V. V. Nemov[1,2], S. V. Kasilov[1,2], W.Kernbichler[2], B. Seiwald[2], Y. Suzuki[3], J. Geiger[4]

[1]*Institute of Plasma Physics, National Science Center "Kharkov Institute of Physics and Technology", Ukraine*

[2]*Association EURATOM-ÖAW, Institut für Theoretische Physik-Computational Physics, TU Graz, Austria*

[3]*National Institute for Fusion Science, Japan*

[4]*Association EURATOM-IPP Greifswald, Germany*

Introduction

In numerical studies of plasma confinement in stellarators it is desirable to use the most realistic magnetic field of the device. Especially, this is necessary for a final stage where it is desirable to use real-space configurations and to take finite plasma pressure and external currents into account. As of today, there exist two three-dimensional MHD finite beta equilibrium codes, PIES [1] and HINT [2], which are used for stellarator plasma equilibrium studies in real-space coordinates. These codes were developed without the a priori assumption of nested magnetic surfaces. However, the requirement of large computer resources (large amount of memory, high speed supercomputers) is characteristic for these codes. Recently, the code HINT has been strongly improved in computational speed, convergence and memory usage, resulting in code HINT2 [3]. The magnetic field, **B**, in HINT2 can be presented in real-space coordinates and it can be conveniently used for an investigation of stellarator confinement properties. In this work, the effective ripple, $\varepsilon_{\rm eff}$, as measure of $1/\nu$-transport is computed for W7-AS and W7-X equilibria with various average β-values. Those equilibrium data are provided as output from the HINT2 code. The $\varepsilon_{\rm eff}$ computations are performed using the code NEO [4].

Magnetic field data and magnetic surfaces

Here, a number of sets of HINT2 data for **B** are used, which had been obtained as results of an equilibrium study for W7-AS with β values of 0.5%, 1.0% and 1.5%, as well as for W-7X with $\beta\approx$2% and $\beta\approx$4%. The HINT2 output for **B** is represented in cylindrical coordinates, ρ,φ,z. The dependencies of B_ρ, B_φ, B_z on ρ,φ and z are given on a three-dimensional grid of discrete mesh points. Between these mesh points the **B** components can be computed using an interpolation procedure. For this procedure either three-dimensional cubic splines or Lagrange polynomial interpolation are used.

The magnetic surfaces obtained as results of a field line following code are presented in Figs. 1 and 2 for W7-AS ($\beta = 0.5\%$ and 1.5%) and W7-X (for $\beta\approx$ 2% and 4%), respectively. It follows from Fig. 1 that for W7-AS with increasing β inner islands corresponding to $\iota = 5/9$ (ι is the rotational transform) and corrugation of the outer magnetic surfaces are increasing. In addition, the magnetic axis is slightly shifted towards the outer side of the torus. The magnetic configuration for $\beta = 1\%$ is not shown in Fig. 1 since it is of intermediate character with respect

*This work, supported by the European Communities under the contract of Association between EURATOM and the Austrian Academy of Sciences, was carried out within the framework of the European Fusion Development Agreement. The views and opinions expressed herein do not necessarily reflect those of the European Commission. Additional funding is provided by the Austrian Science Foundation, FWF, under contract number P16797-N08.

to the presented configurations. One can note that the shapes of the presented magnetic surface cross-sections are qualitatively in good agreement with results for configurations having a boundary ι-value of $5/9$ in Refs. [5] and [6].

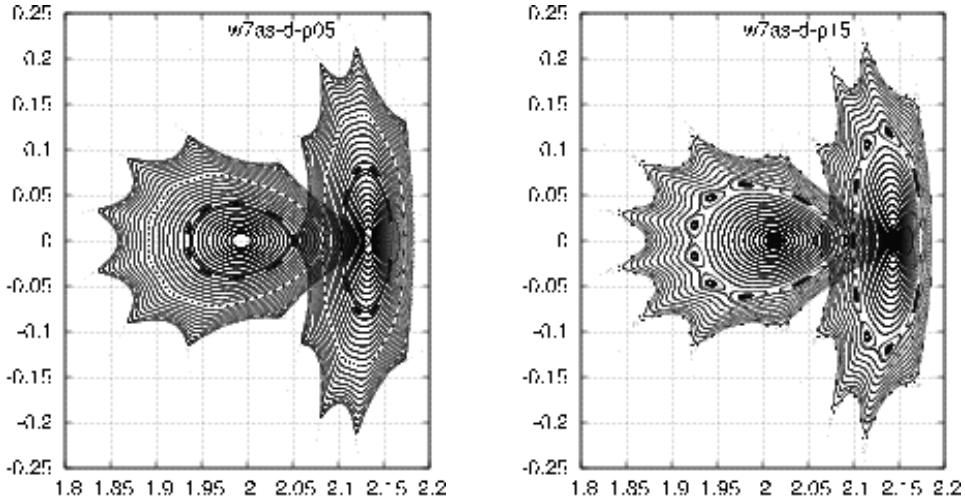

Fig. 1. Magnetic surfaces of W7-AS in the $\varphi = 0$ plane and after a half of the field period for $\beta = 0.5\%$ (left, "w7as-d-p05") and $\beta = 1.5\%$ (right, "w7as-d-p15"). Sizes are given in meters.

From Fig. 2 it can be seen that in W7-X the confinement region (shown in black) is surrounded by a stochastic region (shown in red) which contain rather big magnetic islands with $\iota = 5/5$. Close to the boundary of the confinement region, small magnetic islands are seen which are smaller for $\beta \approx 2\%$. For $\beta \approx 4\%$ the results in Fig. 2 are in good agreement with the results for the finite β equilibrium of the high mirror configuration ($\beta \approx 4.36\%$) in Ref. [7].

Effective ripple computations

To study the $1/\nu$ transport for these configurations the numerical field line following code NEO [4] is used. For an arbitrary stellarator type magnetic field, this code computes the parameter $\varepsilon_{\rm eff}^{3/2}$ with $\varepsilon_{\rm eff}$ being the so called equivalent helical or effective ripple. The $1/\nu$ transport coefficients are proportional to $\varepsilon_{\rm eff}^{3/2}$ and it is the part which contains all the influence of the magnetic field geometry.

The computational results for $\varepsilon_{\rm eff}^{3/2}$ are presented in Fig. 3 (left) as functions of the distance, ξ, of starting points of integration from the magnetic axis in the $\varphi = 0$ plane. Starting points for every magnetic surface are chosen in the $\varphi = 0$ plane at the outer side of mid plane with respect to the magnetic axis. The results are obtained for integration intervals corresponding to 250 field periods for intact magnetic surfaces and to 3000 field periods for island and near island magnetic surfaces. It follows from the results that $\varepsilon_{\rm eff}^{3/2}$ values for W7-AS are rather small near the magnetic axis. With increasing ξ these values are increasing and come close to the level for stellarators which are not-optimized with respect to neoclassical transport (see, e.g., [4]). In this outer region they are much bigger than those for W7-X (plots 4 and 5 in Fig.3). With increasing β $\varepsilon_{\rm eff}^{3/2}$ for W7-AS also increases. For W7-X, $\varepsilon_{\rm eff}^{3/2}$ is somewhat bigger for $\beta \approx 2\%$ than for $\beta \approx 4\%$ in the central part of the confinement regions. The boundaries of the confinement region are $\xi \approx 0.2$ ($\beta \approx 4\%$) and $\xi \approx 0.24$ ($\beta \approx 2\%$). In the stochastic regions at higher ξ much larger $\varepsilon_{\rm eff}^{3/2}$ results are obtained which are shown conditionally with rhombi. However, when the starting points of integration fall into regions of islands at $\iota = 5/5$, big but finite values of $\varepsilon_{\rm eff}^{3/2}$ are obtained. Within the confinement regions, for W7-AS as well as

for W7-X irregularities of $\varepsilon_{\rm eff}^{3/2}$ are seen for island magnetic surfaces and in their vicinity. For W7-X this effect is more pronounced in the $\beta \approx 4\%$ case.

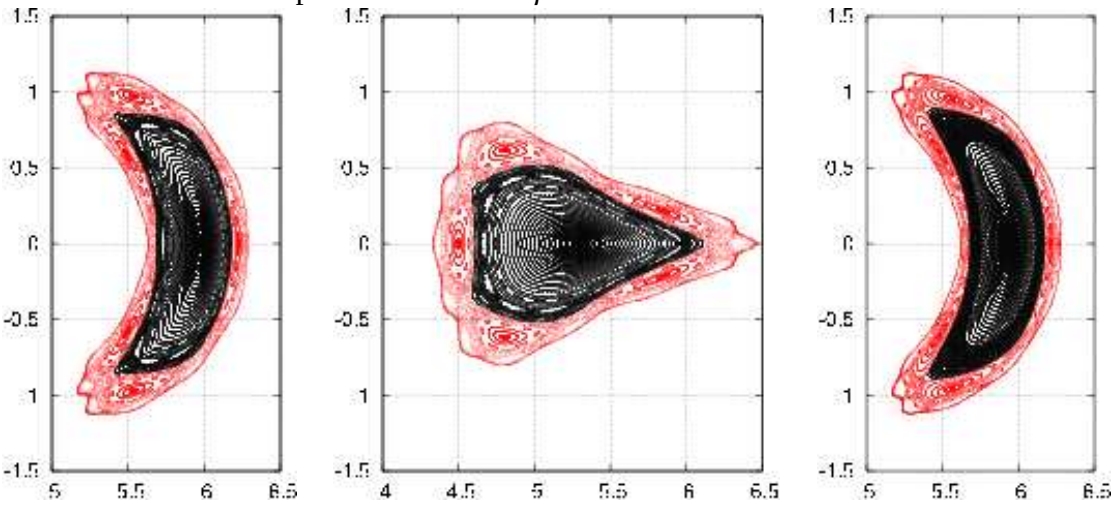

Fig.2. Magnetic surfaces of W-7X in the φ=0 plane (left, right) and after a half of the field period (middle) for $\beta\approx$4% (left, middle) and $\beta\approx$2% (right). Sizes are given in meters.

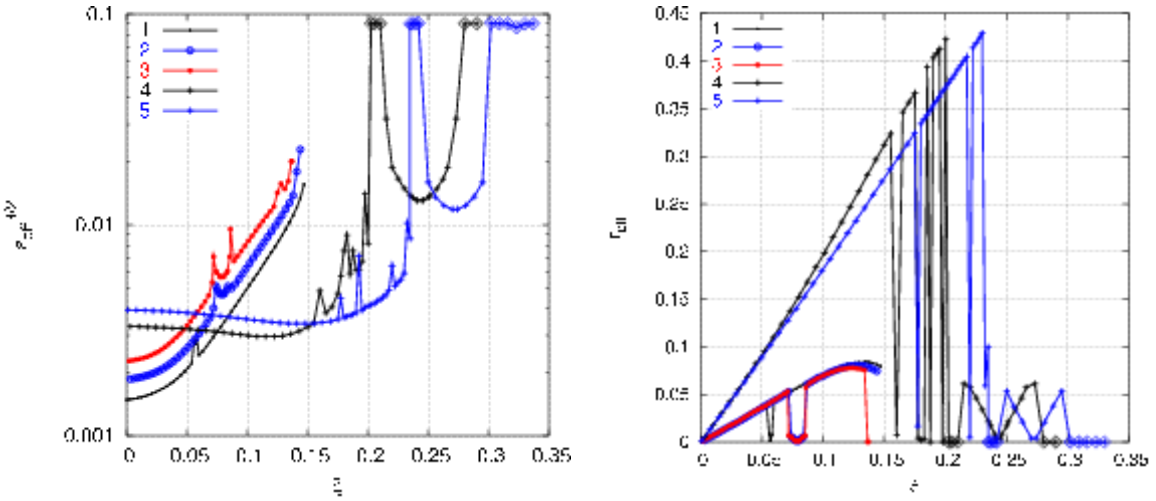

Fig.3. Parameters $\varepsilon_{\rm eff}^{3/2}$ (left) and $r_{\rm eff}$ (right) as functions of ξ=$R_{st} - R_{ax}$; 1: W7-AS, $\beta = 0.5\%$, $R_{ax} \approx 1.994$ (black); 2: W7-AS, $\beta = 1.0\%$, $R_{ax} \approx 2.003$ (blue); 3: W7-AS, $\beta = 1.5\%$, $R_{ax} \approx 2.013$ (red); 4: W7-X, $\beta \approx 4\%$, $R_{ax} \approx 5.98$ (black); 5: W7-X, $\beta \approx 2\%$, $R_{ax} \approx 5.94$ (blue); rhombi mark stochastic regions in W7-X. R_{st} and R_{ax} are starting point of integration and magnetic axis position, resp., in the $\varphi = 0$ plane.

Effective radius

Together with $\varepsilon_{\rm eff}^{3/2}$, an auxiliary parameter $r_{\rm eff}$ is also calculated. This parameter is defined as

$$r_{\rm eff} = \frac{2V}{S}, \tag{1}$$

with

$$\frac{V}{S} = \frac{1}{3} \lim_{L_s \to \infty} \left(\int_0^{L_s} \frac{ds}{B} \mathbf{r} \cdot \nabla \psi \right) \left(\int_0^{L_s} \frac{ds}{B} |\nabla \psi| \right)^{-1}. \tag{2}$$

Here, S is the magnetic surface area and V is the volume enclosed by this surface. The ratio V/S is computed using integration over the magnetic field line length, s, as it is seen from (2),

where ψ is the magnetic surface label and **r** is the radius vector. The integration interval is the same as for $\varepsilon_{\rm eff}^{3/2}$ computations. The computational results for $r_{\rm eff}$ are presented in Fig. 3 (right). For magnetic surfaces with nearly circular cross-sections, $r_{\rm eff}$ is close to the mean radius of the magnetic surface cross-section. In general, $r_{\rm eff}$ is a convenient approximation of this quantity. However, such an estimate can not be valid for complicated shapes of magnetic surfaces. It is seen from Fig. 3 that for W7-AS when approaching the plasma edge $r_{\rm eff}$ decreases whereas the mean radius of the magnetic surface cross-section should increase there. The reason for this is the fact that the area S increases faster than V because of increasing corrugation of the magnetic surface shape (see Fig. 1). In addition, rapid drops of $r_{\rm eff}$ in Fig. 3 are clear signs of magnetic islands.

Note that with increasing V the energy content of the plasma is increasing. At the same time the energy losses are increasing with increasing S. Therefore, the V/S ratio can be considered as an additional parameter for stellarator optimization. An increase of V/S corresponds to a better optimization and a decrease of $r_{\rm eff}$ in the vicinity of the plasma boundary is an undesirable effect from this viewpoint.

Summary

For the analysis five sets of HINT2 data for **B** are used, which had been obtained as results of an equilibrium study for W7-AS with β values of 0.5%, 1.0% and 1.5% (boundary ι of 5/9 [5,6]), as well as for W7-X with $\beta \approx 2\%$ and $\beta \approx 4\%$ (high mirror configuration [7]). The HINT2 output for **B** is given in cylindrical coordinates, ρ, φ, z. The dependencies of B_ρ, B_φ, B_z on ρ, φ and z are given on a three-dimensional grid of discrete mesh points. Between these mesh points the **B** components were computed using interpolation either by three-dimensional cubic splines or Lagrange polynomial interpolation. From the computational results it follows that for W7-AS configurations $\varepsilon_{\rm eff}^{3/2}$ increases with increasing β. For W-7X, $\varepsilon_{\rm eff}^{3/2}$ is somewhat bigger for $\beta \approx 2\%$ than for $\beta \approx 4\%$. An increase of $\varepsilon_{\rm eff}^{3/2}$ is found for magnetic islands and for non-island magnetic surfaces which are close to islands. One has also to note that an undesirable effect of a decrease of the V/S-ratio takes place for W7-AS in the vicinity of the plasma boundary.

The obtained results demonstrate the possibility of using HINT2 data for study of neoclassical transport in stellarators.

References

[1] A. H. Reiman and H. Greenside, J. Comput. Phys. **75**, 423 (1988)

[2] K. Harafuji, et al., J. Comput. Phys. **81**, 169 (1989)

[3] Y. Suzuki, et al., Nucl. Fusion **46**, L19 (2006)

[4] V. V. Nemov, S. V. Kasilov, W. Kernbichler and M. F. Heyn, Phys. Plasmas, **6**, 4622 (1999).

[5] J. Geiger, T. Hayashi, Proc. 29th EPS Conf. on Plasma Phys. and Contr. Fusion (Montreux), 17-21 June 2002 ECA Vol.**26B**, P-5.035 (2002).

[6] J. Geiger, Y. Suzuki, Proc. 33rd EPS Conf. on Plasma Phys. Rome, 19-23 June 2006 ECA Vol.**30I**, P-2.115 (2006).

[7] Y. Suzuki, 2nd Joint meeting of US-JAPAN Workshop and Kyoto University 21st Century COE symposium on "New approaches in plasma confinement experiments in helical systems", Nov. 13-15, 2006.